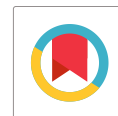# Eco-friendly Synthesis of Ferric Oxide Nanoparticles - Antimicrobial Activity

M. Vishalatchi, V. Kalaiselvi[*], P. Yasotha, B. Blessymol
Department of Physics, Navarasam Arts and Science College for Women, Arachalur, Erode, TN, India

*nk.arthi.kalai@gmail.com

ABSTRACT

Ferric oxide nanoparticles were synthesized by eco-friendly green synthesis and chemical synthesis methods. FeO nanoparticles were synthesized by Chemical co-precipitation method associated with microwave irradiation method and were characterized by XRD, FTIR, SEM, EDAX and Antibacterial Activity. The X-ray Diffraction (XRD) pattern analysis has revealed the crystal structure of FeO. The FTIR pattern has represented the functional groups of the prepared sample. The morphology and purity of the samples were analyzed by using Scanning Electron Microscopy and Energy Dispersion X-ray Diffraction analysis. The Antibacterial activity of the FeO nanoparticles were tested with gram positive *Staphylococcus aureus* and *Bacillus subtilis,* gram negative *Escherichia coli* and *Pseudomonas aeruginosa*. The results matched well with the standard values.

Keywords: Ferric oxide; Antibacterial activity; Papaya leaf; Local and hill station.

1. INTRODUCTION

Nanomaterials are the materials which have at least one dimension between 1-100 nm. Nanomaterials have several applications such as data storage, functional devices and communications (Gentile *et al.* 2016). The iron and oxygen composed to form iron oxides. Iron (III) oxide or Ferric oxide is an inorganic compound with chemical formula Fe_2O_3 (Mohammadi *et al.* 2012). Papaya, generic name of the tree, and the fruit carica papaya have various traditional and ethnic applications both in food and medicinal fields. The most important biologically active compounds in papaya are polyphenol. They are responsible for almost all pharmacological activities due to their anti-oxidant and anti-bacterial properties (Rahman *et al.* 2011).

2. MATERIALS AND METHODS

2.1 Materials

Ferric chloride, sodium hydroxide pellets and distilled water were purchased from Merck in Erode, Tamilnadu, India. Carica papaya leaves (capping agent), were collected from Erode district and Guddalore, India.

2.2 Synthesis of Pure FeO Nanoparticles

Ferric oxide nanoparticles (FeO NPs) were synthesized by microwave irradiation method. For this preparation, ferric chloride ($FeCl_3$) was dissolved in distilled water, and the solutions was stirred for 30 minutes and mixed well. Sodium hydroxide, dissolved in water, was added to ferric chloride solution. The solution was placed over a night and the deposited sample was washed several times in distilled water. The deposited sample was transferred into microwave oven to remove the surrounding water product by drying process for a few minutes. Then, the produced precipitate was calcined at 400 °C for 2 h. The resultant powder of FeO NPs thus obtained was used for subsequent characterization.

2.3 Green Synthesis of Pure FeO NPs using Carica Papaya Leaves

For green synthesis process, the papaya leaves were collected from local and hill station areas. The solution was prepared by dissolving ferric chloride ($FeCl_3$) in distilled water, and the solution was stirred for 30 minutes and mixed well. Meanwhile, 30 g of papaya leaf was mixed with 100 ml of water, and heated until the leaf extract was obtained. Sodium hydroxide was dissolved in water and the solution was added to ferric chloride solution. The solution was placed over a night and the deposited sample was washed several times in distilled water. The deposited sample was transferred into microwave oven to remove the surrounding water product by drying process at maximum power for a few minutes. The resultant powder of FeO NPs thus obtained was used for subsequent characterization.

The synthesized samples shall be designated as FeO for pure iron oxide nanoparticles, LPO for iron oxide nanoparticles synthesized using local area papaya leaves and HPO for iron oxide nanoparticles synthesized using hill station papaya leaves.

3. CHARACTERIZATION TECHNIQUES

3.1 XRD Analysis

X-ray diffraction measurement of prepared samples were determined by an X' Pert Pro P Analytical X-ray Diffractometer instrument. Lattice parameters (a and c), unit cell volume and crystalline size of the sample were determined from the XRD pattern (Olimpia *et al.* 2021).

3.2 SEM Analysis

Scanning Electron Microscope (SEM) has the capacity to produce high resolution images of a sample surface. SEM images have a characteristic three-dimensional appearance and are very useful for judging the surface structure of the sample (Karthika *et al.* 2021).

3.3 EDAX Analysis

EDAX Analysis was used to determine the chemical composition of unknown materials; it was used to identify the chemical composition of the prepared samples (Dawoud and Shaat, 2006).

3.4 FTIR Analysis

The chemical bonding, molecular structure of materials, organic- and inorganic-related information can be collected by Fourier Transform Spectrometer. It is also used to understand the structure of individual molecules and the composition of molecular mixtures in industry and academic laboratories (Kalaiyan *et al.* 2020).

3.5 Antimicrobial Activity

Antimicrobial activity was carried out for the prepared powder samples against gram-positive bacteria, *Staphylococcus aureus* and *Bacillus subtilis* and gram-negative bacteria, *Escherichia coli* and *Pseudomonas aeruginosa*.

4. RESULTS AND DISCUSSION

4.1 XRD Analysis

XRD pattern has revealed the grain size of the sample. The crystalline size of nanoparticle was determined by peak values. The crystalline size was calculated by the Debye-Scherrer formula,

$$D = K\lambda/\beta\cos\theta$$

where,

K $\longrightarrow$ is the constant = 0.9

λ $\longrightarrow$ is the X-ray wavelength

β $\longrightarrow$ is the full width half maximum [FWHM] of the peak in XRD pattern

θ $\longrightarrow$ is the Bragg's angle

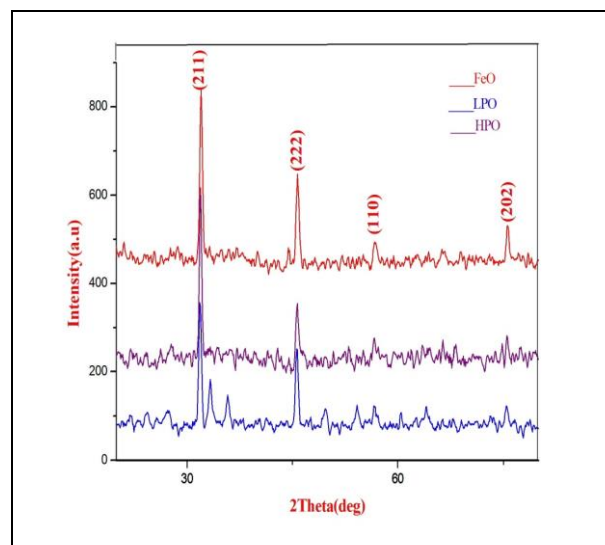The capping of leaf extract enhances the property by decreasing the crystalline size in the sample.

Fig 1: XRD pattern of FeO, LPO and HPO NPs

Table 1: XRD region of FeO, LPO and HPO NPs

Sample	2Θ (deg)	D spacing Å	hkl value	Crystalline size (nm)
FeO	32.06	2.80	211	18.12
	45.76	1.98	222	19.93
LPO	56.80	1.62	110	18.33
HPO	75.57	1.25	202	19.01

The XRD pattern of prepared FeO, LPO and HPO were shown in Fig 1. The prepared samples have peak values for 2θ = 32.06, 45.76, 56.0 and 75.57. The indexed hkl planes are (211), (222), (110) and (202). The average crystalline size of FeO, LPO and HPO was 18.8 nm.

4.2. SEM Analysis

The SEM image of the pure FeO nanoparticles and green synthesis of LPO and HPO nanoparticles were shown in Fig. 2 (a), (b) and (c). Pure FeO (Fig. 2a) sample has shown sphere-shaped nanoparticles. Green synthesis of LPO has shown the spherical twisted nanoparticles (Fig. 2b). Similarly green synthesis of HPO (Fig. 2c) has shown sphere-shaped nanoparticles.
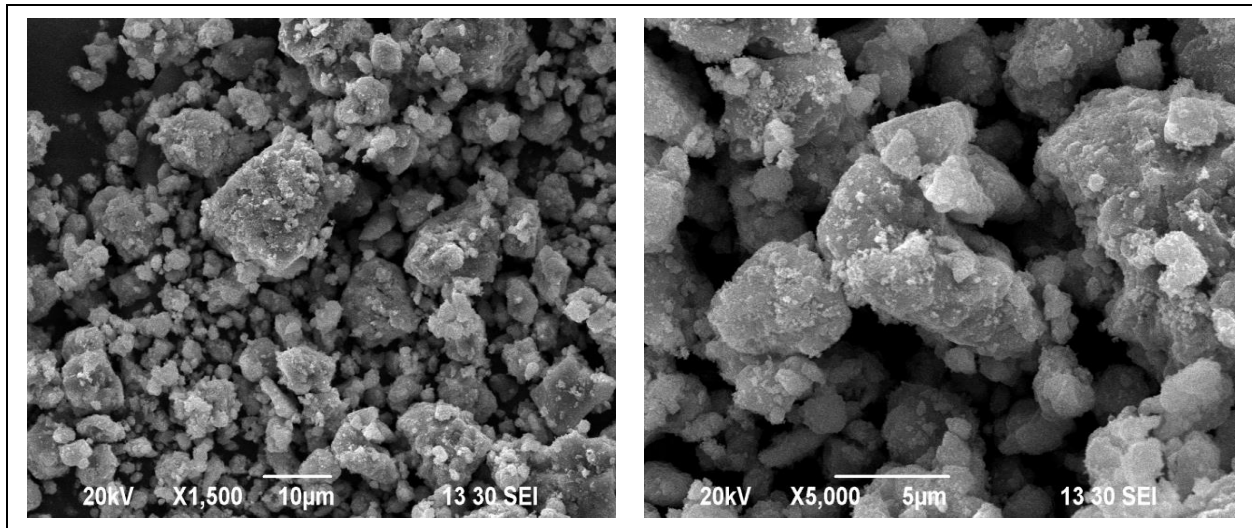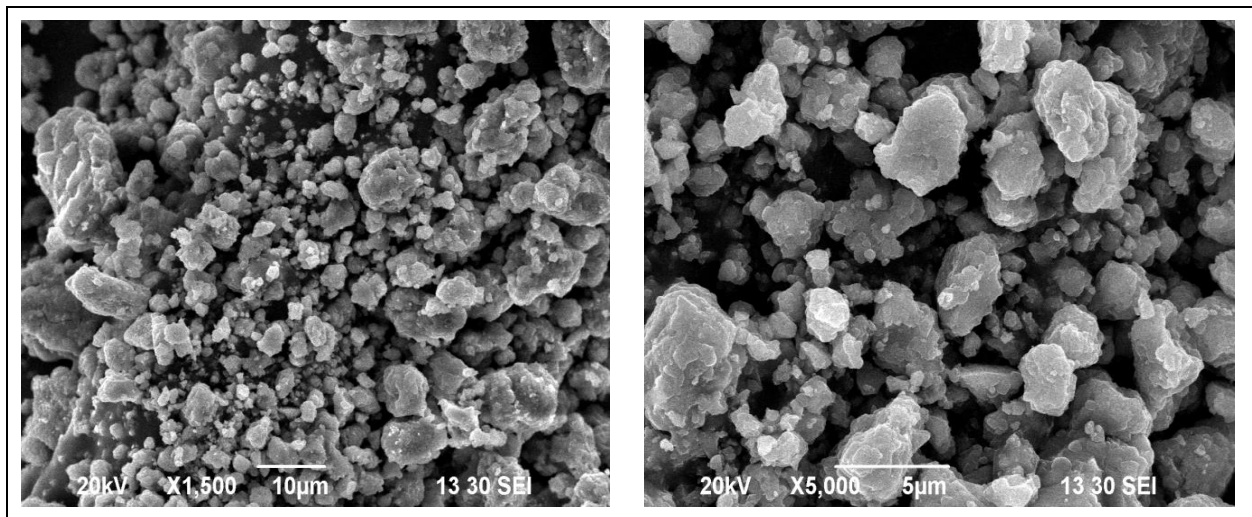
Fig. 2(a): SEM image of pure FeO NPs

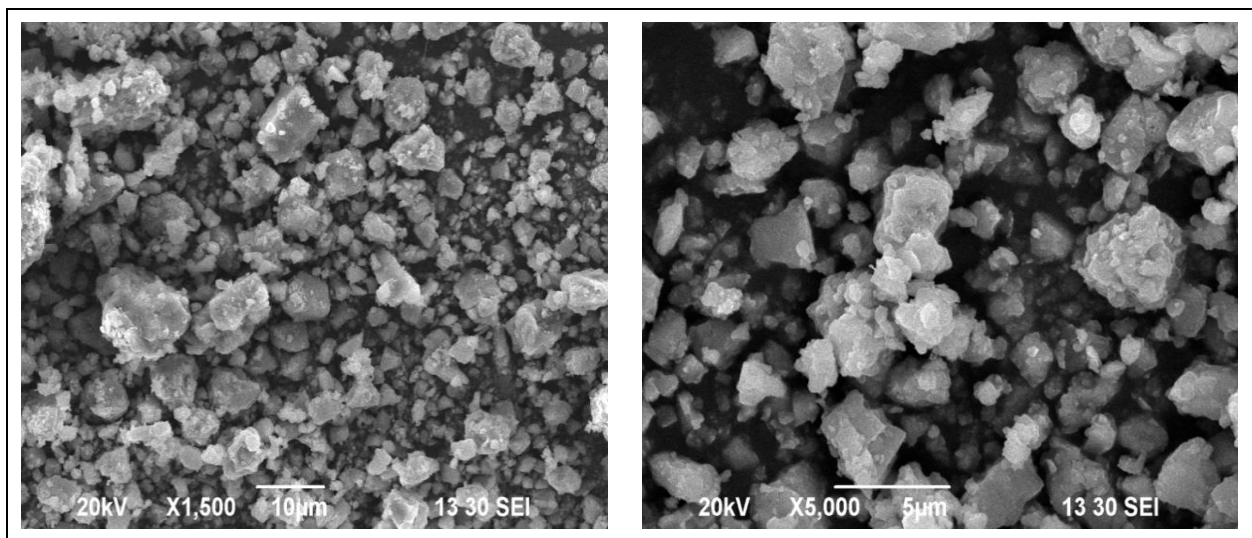**Fig. 2(b): SEM image of LPO NPs**

Fig. 2(c): SEM image of FeO with HPO NPs

The SEM image of FeO and LPO nanoparticles have revealed the sphere-shaped image but the HPO sample has shown cluster-shaped image. Thus, iron oxide with LPO has a perfect shape and hill station papaya leaf was not perfectly associating with iron oxide.

4.3 EDAX Analysis

EDX analysis was used to measure the chemical composition present in the sample. The EDX examination consisted of spectra showing peaks corresponding to the elements making up the true composition of the sample, as shown in Fig. 3(a), (b) and (c).
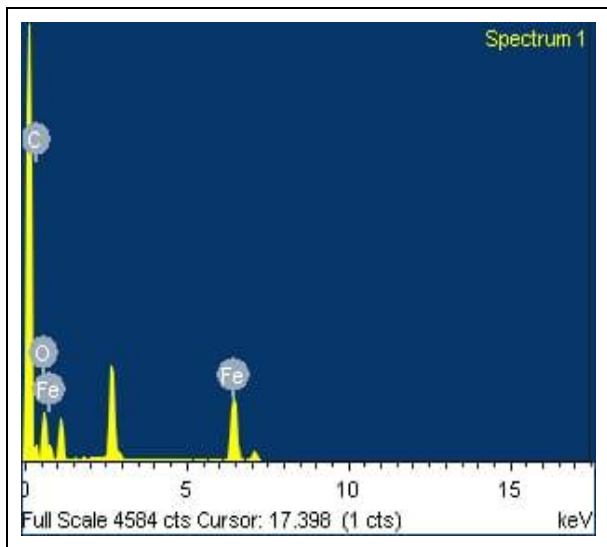

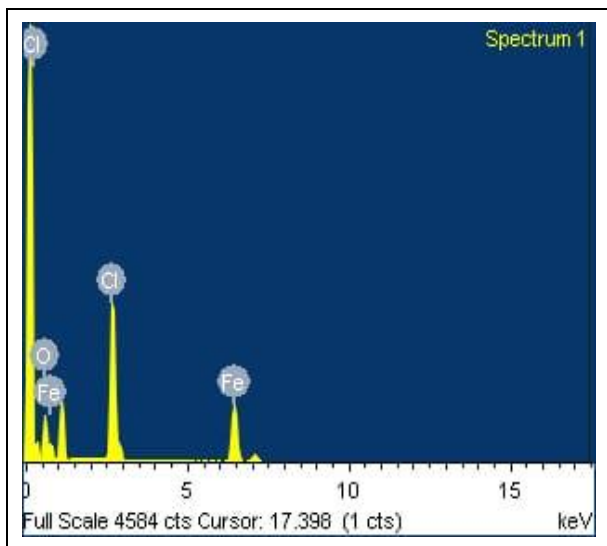**Fig. 3(a): EDX spectra of pure FeO**
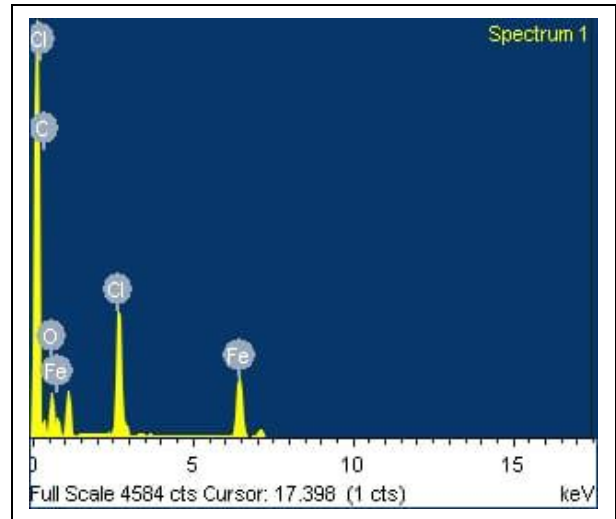

Fig. 3(b): EDX spectra of LPO

Fig. 3(c): EDX spectra of HPO

Table 2(a). EDX analysis of FeO

Element	Intensity	Weight %	Atomic Weight %
O	0.8131	35.95	60.64
Cl	0.8546	30.23	23.01
Fe	0.8809	33.82	16.34

Table 2(b). EDX analysis of LPO

Element	Intensity	Weight %	Atomic Weight %
C	0.5718	16.92	32.10
O	1.1459	33.45	47.64
Fe	0.8851	49.64	20.26

Table 2(c). EDX analysis of HPO

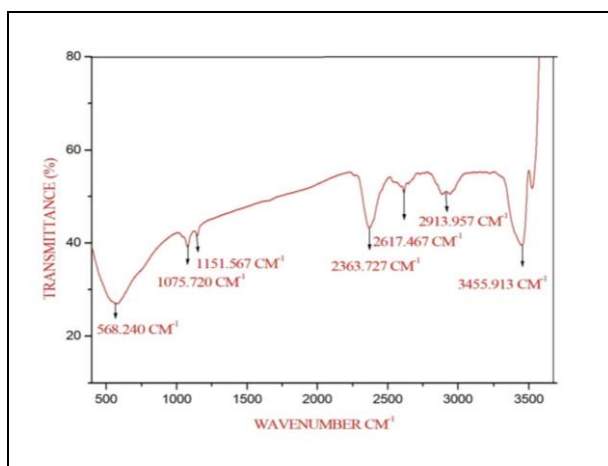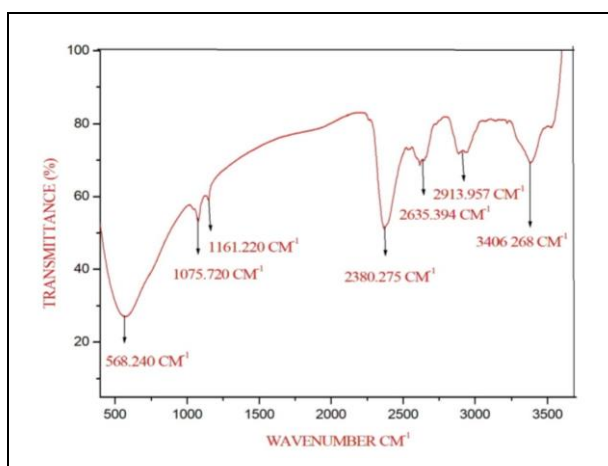| Element	Intensity	Weight %	Atomic Weight %
C	0.2084	2.86	6.31
O	0.8573	34.61	57.25
Cl	0.8464	24.95	18.63
Fe	0.8837	37.58	17.81

Fig 4(a): FTIR analysis of FeO NPs

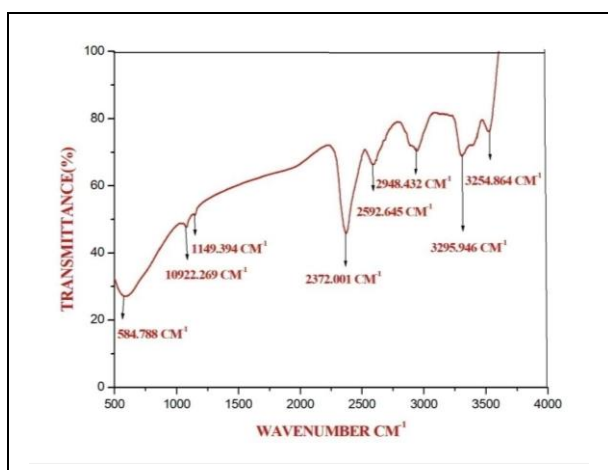**Fig 4(b): FTIR analysis of LPO NPs**

Fig 4(c): FTIR analysis of HPO NPs

From the analysis, only Fe (Iron), Cl (Chlorine) and O (Oxygen) were observed in pure FeO samples. In LPO and HPO samples, Fe (Iron), Cl (Chlorine), O (Oxygen) and C (Carbon) were found. The presence of carbon has revealed the incorporation of papaya extract

in the samples. This represents the purity of the sample shown in Fig 3. In EDAX, the presence of carbon has revealed the incorporation of capping agent in the sample.

4.4 FTIR Analysis

The FTIR studies have revealed the presence of various functional groups in pure FeO, LPO and HPO.

In pure FeO (Fig. 4a) and FeO with local area papaya (Fig. 4b), the absorption spectra of 568.240 cm^{-1} point out the presence of C-l stretching. 1075.720 and 1151.567 cm^{-1} and also 1161.220 cm^{-1} have shown the presence of C-O stretching. The mode of vibration at 2363.727 cm^{-1} and 2380.275 cm^{-1} have represented the presence of O=C=O stretching. The vibration mode at 2617.467 cm^{-1} and 2635.394 cm^{-1} have revealed the presence of S-H stretching; 2913.957 cm^{-1} has revealed the presence of C-H stretching. The spectra of 3455.913 and 3406.268 cm^{-1} have shown the presence of O-H stretching (Sekar *et al* 2020).

In HPO, shown in Fig 4(c), the absorption spectrum of 584.788 cm^{-1} has indicated the presence of C-l stretching. 1092.269 cm^{-1} and 1149.349 cm^{-1} have shown the presence of C-O stretching. The mode of vibration at 2372.001 cm^{-1} has represented the presence of O=C=O stretching. The vibration mode at 2592.645 cm^{-1} has revealed the presence of S-H stretching; 2948.432 cm^{-1} has revealed the presence of C-H stretching. The spectrum of 3295.946 cm^{-1} and 3254.864 cm^{-1} have shown the presence of O-H stretching.

The highest one observed at 568 cm^{-1} was corresponding to intrinsic stretching vibration of Fe↔O. The region of peaks, 1500-950 cm^{-1}, is called fingerprint region for FTIR spectra of tannins. The peak at 2372.0 cm^{-1} was due to O=C=O stretching, owing to the effect of polyphenols and natural pigment from the plant leaf extracts. Introducing capping agent has created a minor change in the functional group analysis of the samples. Thus the FTIR has revealed the existence of various reducing agents and functional groups present in the papaya plant leaf extract. The shift in peak position in the range of 400–4000 cm^{-1} has ensured that these functional groups contain compounds bound to the iron oxide surface (9, 10).

4.5 Antimicrobial Activity

The antimicrobial activity of the nanoparticles was tested against for two gram-positive microorganisms, *Bacillus cereus (MTCC 430)* and *Staphylococcus aureus (MTCC 3160)*, two gram-negative microorganisms, *Escherichia coli (MTCC 1698)* and *Pseudomonas aeruginosa (MTCC10309),* by Agar well diffusion method. Ciprofloxacin was used as the standard for all the samples.

Table 4. FTIR analysis of synthesized samples

Bond Range (cm^{-1})			Stretching			Intensity (Stretching mode)		
FeO	LPO	HPO	FeO	LPO	HPO	FeO	LPO	HPO
568.2	568.2	584.7	Strong	Strong	Strong	C-l	C-l	C-l
1075.7	1075.7	1092.2	Strong	Strong	Strong	C-O	C-O	C-O
1151.5	1161.2	1149.3	Strong	Strong	Strong	C-O	C-O	C-O
2363.7	2380.2	2372.0	Strong	Strong	Strong	O=C=O	O=C=O	O=C=O
2617.4	2635.3	2592.6	Weak	Weak	Medium	S-H	S-H	S-H
2913.9	2913.9	3295.9	Medium	Medium	Strong	C-H	C-H	O-H
3455.9	3406.2	3254.8	Strong	Strong	Strong	O-H	O-H	O-H

Fig. 5(a): Anti-bacterial activity of pure FeO, LPO and HPO NPs against gram-positive (A) S*taphylococcus aureus* and (B) *Bacillus subtilis*

Fig 5(b): Anti-bacterial activity of pure FeO, LPO and HPO against gram-negative (A) *Escherichia coli* and (B) *Pseudomonas aeruginosa*

The antibacterial activity of FeO, LPO and HPO nanoparticles were shown in Fig 5(a and b) and the values were displayed in Table 5.

Thus, FeO and HPO have given good anti-bacterial action against both gram-positive and gram-negative bacteria. The activity against *B. subtilis and S. aureus* was efficient for FeO and HPO samples. There was no ZOI for LPO, as shown in Fig 5. Therefore, the results have shown that the synthesized samples obviously have the anti-bacterial activities, which is the main property of iron oxide. The ZOI for both FeO and

HPO were established; there was a small difference between them. There is no action for LPO which revealed that HPO has great anti-bacterial activity than local papaya leaves with iron oxide. Due to climatic change in hill stations, the plants from hill station have good zone of inhibition against microbes.

Table 5. ZOI of FeO NPs against gram-positive and gram-negative bacteria

Bacteria	Organisms	Ciprofloxacin (100 µg/disc)	Zone of Inhibition (mm) Sample (100 µg/disc)		
			FeO	LPO	HPO
Gram positive	*Staphylococcus aureus*	33	26	-	20
	Bacillus subtilis	28	25	-	16
Gram negative	*Escherichia coli*	34	28	-	18
	Pseudomonas aeruginosa	32	24	-	22

5. CONCLUSION

The iron oxide nanoparticles have been synthesized by using chemical precipitation and green synthesis assisted microwave irradiation method, using capping agent from different localities. The synthesized samples were characterized by using XRD, SEM, EDX, FTIR and Antimicrobial Activity. The XRD pattern has indicated the crystalline size of nanoparticles. The average crystalline size of FeO, LPO and HPO nanoparticles was 18.8 nm. In the presence of papaya leaves, the crystalline size of the sample has shown no change. The SEM analysis has revealed the morphological structure of iron oxide nanoparticle. FeO and LPO have shown the sphere-shaped morphological structure; but HPO has shown a cluster-shaped morphological structure. The EDAX analysis has confirmed the presence of elemental composition in the samples. In FeO, the composition of ferric and oxide groups was in the ratio of 1:4; in LPO and HPO, the compositions were in the ratio of 1:2 and 1:3, respectively. Presence of carbon has indicated the involvement of papaya leaves in the sample. The FTIR spectrum has predicted the presence of functional groups in the sample. It has confirmed the presence of polyphenols and natural pigment groups in the sample. Antimicrobial Activity has predicted the zone of inhibition of the samples. Influence of gram-positive and gram-negative bacteria in FeO and HPO were high compared with LPO. There was no ZOI in LPO; thus, it can be concluded that the chemically prepared iron oxide and green-synthesized iron oxide with papaya leaves can be best used for the anti-bacterial applications.

FUNDING

CONFLICTS OF INTEREST

The authors declare that there is no conflict of interest.

COPYRIGHT

REFERENCE

Gentile, A., Ruffino, F. and Grimaldi, M. G., Complex-morphology metal-based nanostructures: Fabrication, characterization, and applications, *Nano Mater.,* 6(6), 1-33 (2016).
https://doi.org/10.3390/nano6060110

Mohammadi, S. Z., Khorasani, M. M., Jahani, S. and Yousefi, M., Synthesis and characterization of α-Fe$_2$O$_3$ nanoparticles by microwave method, *Int. J. Nanosci. Nanotechnol.*, 8(2), 87-92 (2012).

Rahman, M. M., Khan, S. B., Jamal, A., Faisal, M. and Aisiri, A. M., Iron oxide nanoparticles, *Nano Mater*, Chapter 3, 43-67 (2011).
https://doi.org/10.5772/27698

Olimpia, A. I., Maria, B., Dina, G., Simelda, E. Z., Marius I. C., Mircea, I. P., Daniel, I. H., Nicoleta, G. H., and Mircea, R., A DPPH· Kinetic Approach on the Antioxidant Activity of Various Parts and Ripening Levels of Papaya (*Carica papaya* L.) Ethanolic Extracts, *Plants*, 10(8), 1-14 (2021)
https://doi.org/10.3390/plants10081679

Karthika, V., Ramya, V., Kalaiselvi, V., Shanmathi, S., Synthesis and Characterization of Zinc Oxide Nanoparticles using Justicia Adhatoda Leaf Extract, *Int. J. Adv. Sci. Eng.,* 7(3), 1839-1842 (2021).
https://doi.org/10.29294/IJASE.7.3.2021.1839-1842

Dawoud, H. A. and Shaat, S. K., A structural study of Cu-Zn ferrites by infrared spectra, *J. Al-Aqsa Unv.,* 10(SE), 247-262 (2006).

Kalaiyan, G., Suresh, S., Thambidurai, S., Prabu, K. M., Kumar, S. K., Pugazhenthiran, N. and Kandasamy, M., Green synthesis of hierarchical copper oxide microleaf bundles using Hibiscus cannabinus leaf extract for antibacterial application, *J. Mol. Struct*., 1217, 1-2 (2020).
https://doi.org/10.1016/j.molstruc.2020.128379

Sekar, V., Mani, D., Baskaralingam, V., Shivendu, R., Kalaiselvi, V., Nandita, D., Jingdi, C., and Esteban, F. D., Biogenic preparation and characterization of ZnO nanoparticles from natural polysaccharide Azadirachta indica. L. (neem gum) and its clinical implications, *J. Cluster Sci.,* 32, 983–993 (2021).
https://doi.org/10.1007/s10876-020-01863-y